Gold Nanocluster-DNase 1 Hybrid Materials for DNA Contamination Sensing

Abby L. West,[1a] Mark H. Griep,[1] Dan P. Cole[2] and Shashi P. Karna[1], senior IEEE member
[1]US Army Research Laboratory, ATTN: RDRL-WM, Aberdeen Proving Ground, MD 21005
[2]US Army Research Laboratory, ATTN: RDRL-VT, Aberdeen Proving Ground, MD 21005
Email: abby.west2.ctr@mail.mil; mark.h.griep.civ@mail.mil; daniel.p.cole.ctr@mail.mil; shashi.p.karna.civ@mail.mil

Abstract –**Protein encapsulated gold nanocluster (P-AuNC) synthesis was first demonstrated in 2009.[1] Initially these P-AuNCs were used as cellular imaging agents as the protein shell surrounding the AuNC made them highly biocompatible. However, recent studies have begun to show that these stabilizing proteins may also retain native biological function thus giving a dual functionality to these hybrid molecules. Here we present the synthesis of DNase 1 stabilized gold nanoclusters (DNase 1:AuNCs) with core sizes consisting either 8 or 25 atoms. The DNase 1:Au_8NCs exhibit blue fluorescence whereas the DNase 1:Au_{25}NCs are red emitting. Moreover, in addition to the intense fluorescence emission; the synthesized DNase 1:AuNC hybrid retain the native functionality of the protein, allowing simultaneous detection and digestion of DNA with a detection limit of 2 μg/mL (Scheme 1). The DNase 1:AuNCs could be conveniently employed as efficient and fast sensors to augment the current inefficient and time consuming DNA contamination analysis techniques.**

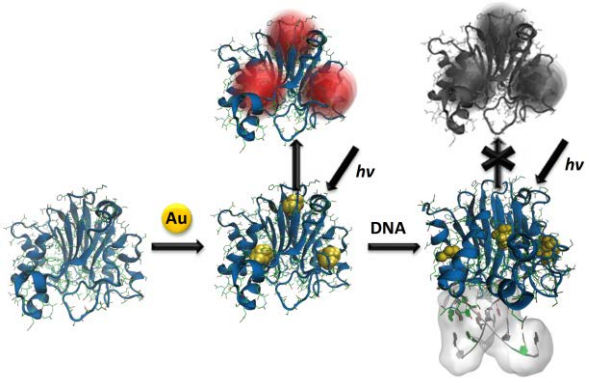

Scheme 1. Schematic of the formation of DNase 1:AuNCs and the DNA mediated quenching of NC fluorescence.

I. Introduction

Fluorescent noble metal nanoclusters possess great promise in the field of biosensing, biodetection and biomedicine.[2, 3] Nanoclusters are small clusters of metal atoms with a diameter of less than 2 nm.[3] This diameter approaches the Fermi wavelength of electrons and therefore the clusters demonstrate molecular-like transitions between their HOMO and LUMO energy levels as opposed to the plasmonic transitions exhibited by nanoparticles (**Figure 1**). [4, 5]

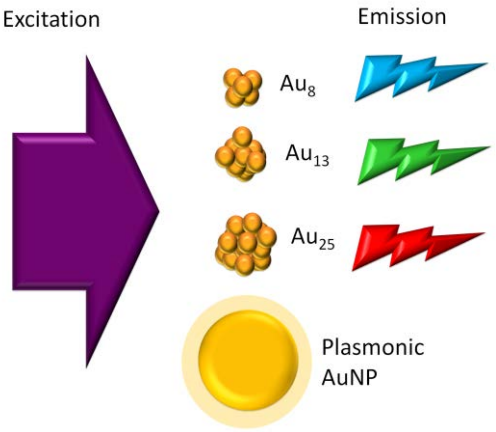

Figure 1. Comparison of the molecular-like discrete transitions exhibited by AuNCs to the plasmonic transitions of AuNPs.

Due to these unique energy transitions, nanoclusters are photoluminescent and the maximum fluorescent emission wavelength is dictated by the size of the cluster.[6] As a result, these discrete energy levels allow for tuneable photonic emission in the visible and IR regions, highly efficient two-photon absorption, and quantum yields comparable to semiconductor QDs. [3, 4, 7] The unique properties of noble metal nanoclusters make them attractive for a numerous applications in a variety of research fields ranging from biologics to optics and photovoltaics.[3, 8-16] Protein mediated nanoclusters have been prepared with several proteins

Report Documentation Page

Form Approved
OMB No. 0704-0188

1. REPORT DATE	2. REPORT TYPE	3. DATES COVERED
2014		**00-00-2014 to 00-00-2014**

4. TITLE AND SUBTITLE	5a. CONTRACT NUMBER
Gold Nanocluster-DNase 1 Hybrid Materials for DNA Contamination Sensing	5b. GRANT NUMBER
	5c. PROGRAM ELEMENT NUMBER
6. AUTHOR(S)	5d. PROJECT NUMBER
	5e. TASK NUMBER
	5f. WORK UNIT NUMBER
7. PERFORMING ORGANIZATION NAME(S) AND ADDRESS(ES) **US Army Research Laboratory,,ATTN: RDRL-WM,,Aberdeen Proving Ground,,MD,21005**	8. PERFORMING ORGANIZATION REPORT NUMBER
9. SPONSORING/MONITORING AGENCY NAME(S) AND ADDRESS(ES)	10. SPONSOR/MONITOR'S ACRONYM(S)
	11. SPONSOR/MONITOR'S REPORT NUMBER(S)

12. DISTRIBUTION/AVAILABILITY STATEMENT
Approved for public release; distribution unlimited

13. SUPPLEMENTARY NOTES

14. ABSTRACT

15. SUBJECT TERMS

16. SECURITY CLASSIFICATION OF:			17. LIMITATION OF ABSTRACT	18. NUMBER OF PAGES	19a. NAME OF RESPONSIBLE PERSON
a. REPORT	b. ABSTRACT	c. THIS PAGE			
unclassified	**unclassified**	**unclassified**	**Same as Report (SAR)**	**7**	

including BSA, apo-transferrin, pepsin, lysozyme, insulin, CRABP, DNase 1 and others.[1, 8, 17-22] Protein encapsulated nanoclusters possess many desirable traits such as green synthesis routes, stability, and very high levels of biocompatibility.[3, 12, 23] Recently, some P-NCs such as human apo-transferrin,[19] insulin[20] and horseradish peroxidase[24] have been shown to retain native function, thus offering a multifunctional bionano hybrid system capable of simultaneous visualization and quantification of virtually any targeted biological process.

Here, we present the synthesis and sensing application of DNase 1 stabilized AuNCs. The nanoclusters consist of either 8 or 25 atoms and exhibit intense blue (Au_8) or red (Au_{25}) fluorescence emission, long term stability, and resistance to photobleaching. Moreover, we show that the DNase 1:AuNC hybrid retains the native functionality of DNase 1.

II. EXPERIMENTAL

Synthesis of DNase 1 stabilized AuNCs. DNase 1 from bovine pancreas (Sigma-Aldrich) was resuspended in Milli Q water at a concentration of 20 mg/mL. 2 mL of aqueous solution of $HAuCl_4$ (20, 10, 5 or 1 mM) was added to 2 mL of protein solution under vigorous stirring at 37˚ C. After 5 minutes 200 μL of NaOH (1 M) was added to raise the pH to ~ 12 for the 1, 5, and 10 mM HAuCl4 samples whereas 400 μL of NaOH (1M) was required. The various protein/gold mixtures were then left to react for 12 hours. The solution changed in color from light yellow to various shades of deeper yellow/gold over the course of the reaction. A parallel experiment was set up with 20 mg/mL protein alone as a control. This solution was initially clear and remained so throughout the course of the incubation.

Photophysical measurements. UV-Visible measurements were taken with a Nanodrop 2000c over a wavelength range of 200 to 800 nm. The fluorescence emission spectra were collected with a Horiba Jobin Yvon FluoroLog-3 spectrofluorometer with maximum excitation wavelengths of 365, 395, 450 and 488 nm. The emission spectrum was measured from 400-700 nm. The fluorescence excitation spectra were obtained through the measurement of two different maximum emission wavelengths, namely 460 and 640 nm.

X-Ray photoelectron spectroscopy (XPS). Near-surface compositional depth profiling of the as-deposited coatings was performed using the Kratos Axis Ultra X-ray photoelectron spectroscopy system, equipped with a hemispherical analyzer. A 100 W monochromatic Al Kα (1486.7 eV) beam irradiated a 1 mm × 0.5 mm sampling area with a take-off angle of 90°. The base pressure in the XPS chamber was held between 10^{-9} and 10^{-10} Torr. Elemental high resolution scans for Au_{4f} core level were taken in the constant analyzer energy mode with 160 eV pass energy. The sp^3 C_{1s} peak was used as reference for binding energy calibration.

Transmission electron microscopy (TEM). Morphological studies and elemental characterization of the materials were performed using a field emission TEM (JEOL JEM-2100F TEM/STEM) operated at 200 kV. The TEM system was equipped with an energy dispersive spectroscopy system (INCA 250, Oxford Instruments) and imaging filter (Gatan). Microscopy samples were prepared for analysis through the following steps: (*i*) bulk material ground up using a mortar and pestle, (*ii*) particles dispersed in deionized water and bath sonicated for 15 min, (*iii*) solution pipetted onto TEM grids (ultrathin carbon film on holey carbon support film, 300 mesh, Ted Pella, Inc.), followed by removal of excess solution using a filter paper, (*iv*) samples allowed to dry in air at room temperature for 2 hr.

DNase 1 activity assay. All DNase 1 activity assays were completed in triplicate. A 1 kb dsDNA ladder with sizes ranging from 10 to 0.5 kb (New England Biolabs) was used as a substrate for cleavage by the endodeoxyribonuclease, DNase 1. Enzyme activity assays for both native DNase 1 and DNase 1: AuNCs were carried out in a final volume of 20 μL buffer (100 mM sodium acetate, 6.25 mM magnesium sulfate pH 5.0), containing 2 μg of dsDNA. The reaction was incubated at room temperature for 20 minutes followed by the addition of 2 units of the control enzyme and 4 units of the various DNase 1:AuNC synthesis reactions. This reaction was further incubated for 30 minutes at 37 ˚C and deactivated at 99 ˚C for 1 minute. DNA degradation was analyzed by 2 % agarose gel electrophoresis. To determine the effect of DNA digestion on DNase 1:AuNC fluorescence, NC fluorescence was monitored during DNA addition. In a typical experiment, 300 mL of 20 mg/mL DNase 1:AuNCs in water was added to a 0.5 cm PL Spectrosil far-UV quartz window fluorescence cuvette (Starna Cells). The fluorescence spectrum of the NCs alone was

obtained with an excitation wavelength of 390 nm (10, 5 and 0.5 mM Au(III)) or 490 nm (2.5 mM Au(III)). DNA from calf thymus (Sigma Aldrich) was titrated and the change in fluorescence measured. The decrease in fluorescence at the max emission wavelength was plotted and fitted with a linear regression line.

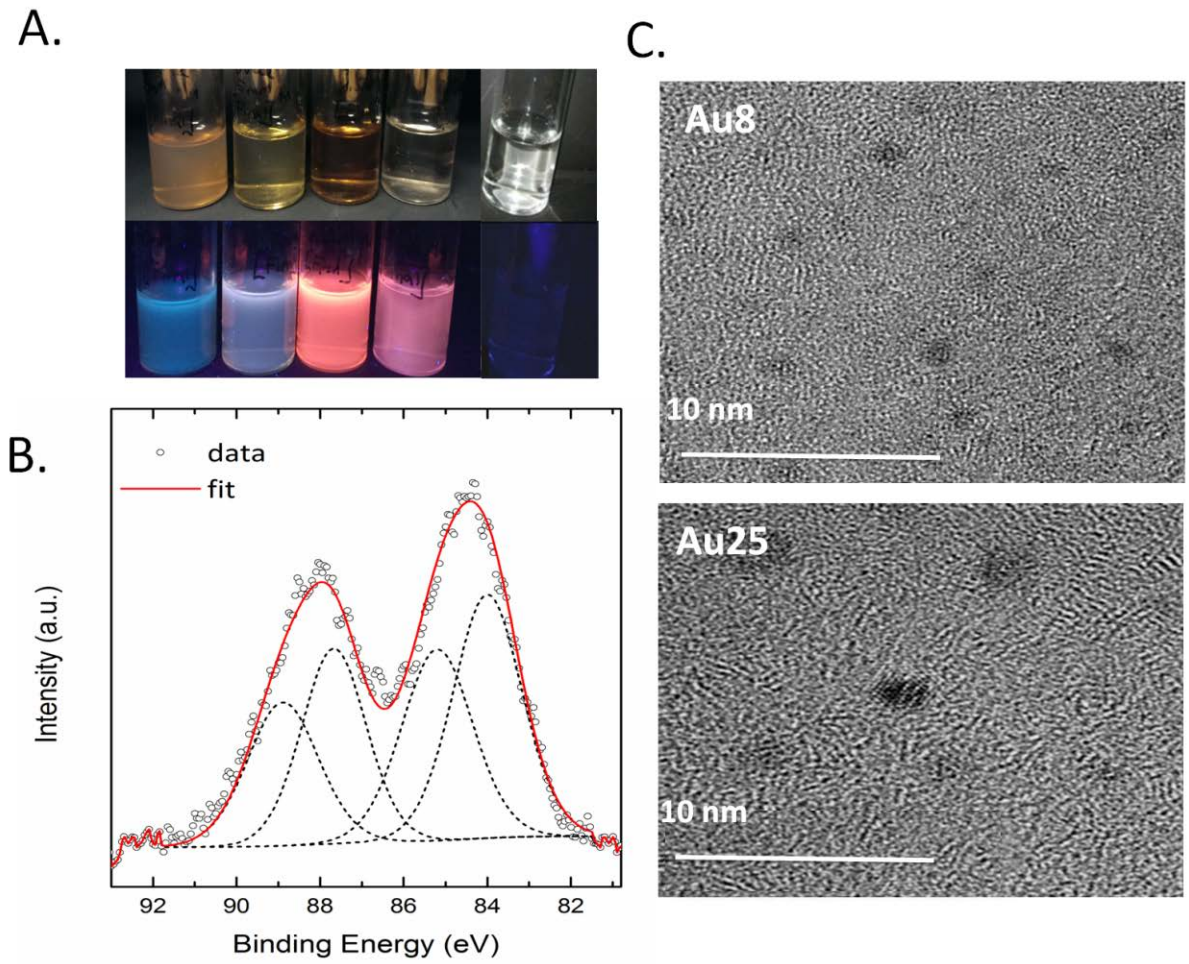

Figure 2. Physical characterization of DNase 1:AuNCs. (A) Visible (top) and UV (bottom) illumination of DNase AuNCs (From left to right: 10, 5, 2.5, 0.5 and 0 mM Au(III) added). (B) XPS data for DNase 1:Au_{25}NCs. Au 4f spectra were fitted and confirm the presence of two distinct doublet Au 4f7/2 peaks at 84 eV and the other at 85.2 eV, corresponding to Au (0) and Au (I) respectively. (C) TEM images of DNase 1:Au_8NCs (Top) and DNase 1:Au_{25}NCs (Bottom).

III. Results and Conclusions

DNase 1 stabilized AuNCs with intense blue or red emission with 10 mM and 2.5 mM $HAuCl_4$ respectively (**Figure 2A**). The other two reactions produced non-optimized slightly fluorescent products. The blue emitting clusters exhibit a max emission wavelength of 460 nm and a max excitation wavelength of 395 nm. According to the study presented by Kawasaki et al[18] and Chen and Tseng [25], a peak emission wavelength of 460 nm is consistent with gold clusters comprised of 8 atoms. The Red emitting clusters exhibit peak fluorescence at 640 nm with a max excitation wavelength of 490 nm which compares well with previously reported P-Au_{25}NCs. The predicted cluster sizes of 8 and 25 atoms were also confirmed with TEM (**Figure 2C**).

In addition to TEM; XPS was performed to determine the ratio of Au(I) ions the form the shell of the clusters and Au(0) that forms the core of the cluster. The ratio of Au(I) to Au(0) should decrease as the cluster core size increases (i.e. from Au_8 to Au_{25}).[18, 25] For example, lysozyme Au_8 clusters are completely comprised of elemental gold (Au(0)) with no Au(I) present on the surface.[25] As such, the DNase 1:Au_{25}NCs should have a higher percentage of oxidized metal than the DNase 1:Au_8NCs. As shown in Figure 3B, the DNase 1:Au_{25}NC XPS spectra of Au 4f spectra were fitted and confirm the presence of two distinct doublet Au 4f7/2 peaks at 84 eV and the other at 85.2 eV, corresponding to Au (0) and Au (I) respectively and show a higher percentage of Au(I) than elemental metal as expected (**Figure 2B**). However, we were unable to successfully acquire XPS spectra of DNase 1:Au_8NCs. It is possible that the XPS instrument we were using was unable to resolve the small clusters or that the sample degraded upon X-Ray exposure.

The blue and red emitting DNase 1:AuNCs were then tested for enzymatic activity. DNase 1 is an endo-deoxyribonuclease that is responsible for the degradation (cleavage) of double stranded DNA (dsDNA) to a smallest unit of 4 base pair segments. DNase 1:AuNCs activity was

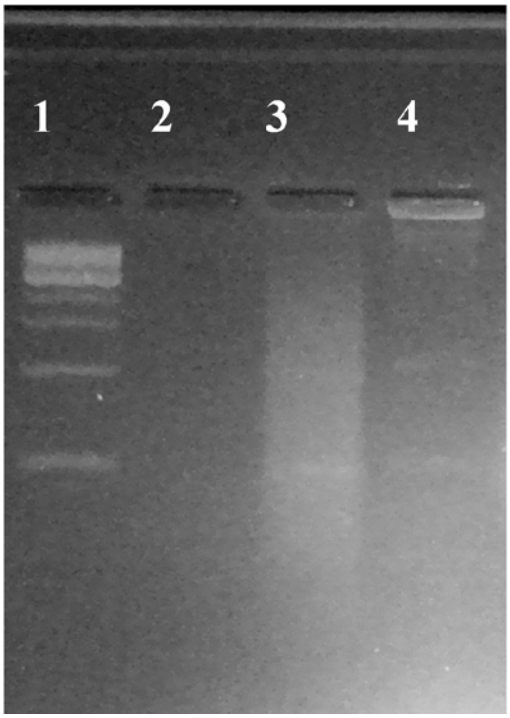

Figure 3. DNase 1 activity assay. Lane 1: blank reaction with dsDNA marker alone. Lane 2: control reaction with stock DNase 1. Lanes 3 and 4: Test reaction with the DNase 1 stabilized Au_8 and Au_{25} clusters. All of the DNase 1:AuNC synthesis products are able to degrade dsDNA.

assayed with two different methods: gel visualization and fluorescence monitoring. The gel visualization approach allows for comparison DNase 1:AuNC enzymatic activities to the native enzyme. DNase 1:Au_8NCs and DNase 1:Au_{25}NCs were incubated with a standard 1 kb dsDNA

ladder and the reaction products were analyzed on an agarose gel. As a control, the dsDNA was also inccubated with the pure enzyme (DNase 1). **Figure 3** shows the results of the agarose gel electrophoresis. As is clear from the gel-electrophoresis columns, both of the DNase 1 stabilized gold nanoclusters were able to degrade the dsDNA template (**Figure 3**, lanes 3-4). Neither of the DNase 1:AuNCs is able to degrade dsDNA to the degree of the control (pristine) enzyme (lane 2), as seen from the slight DNA smearing for the AuNC enzyme compared to no smearing for the enzyme alone. It is also interesting to note that each of the DNase 1:AuNC complex, regardless of the size of the Au clusters (Au_8 or Au_{25}) sppears to degrade dsDNA to the same degree. This is somewhat surprising, since one can expect that the smaller cluster (Au_8), with less propensity to induce structural changes in the stabilizing enzyme would allow a higher degree of enzymatic activity than the larger (Au_{25}) clusters. However, our results clearly demonstrate that, at least between the Au_8 and Au_{25} clusters there is no real difference in the enzymatic activity of the stabilizing protein.

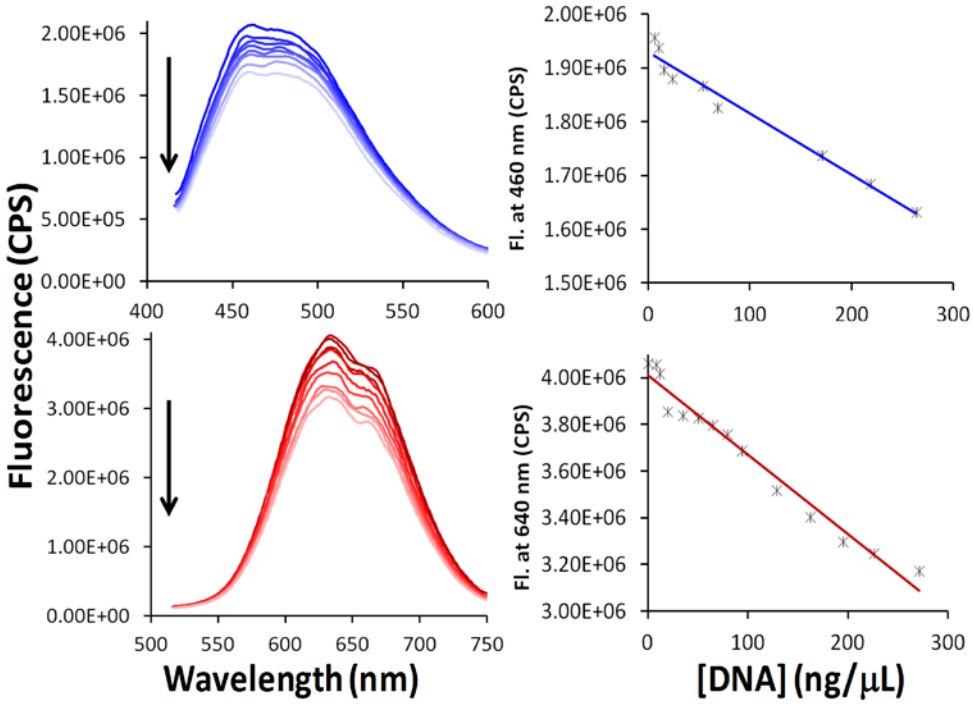

Figure 4. Left panel: Fluorescent responses of DNase 1:Au_8NCs (Top) and DNase:Au_{25}NCs (Bottom) after the addition of DNA (2 - 260 µg/ml). Right panel: Plot of the fluorescence decrease at 460 or 640 nm for the Au_8 and Au_{25} clusters, respectively.

We next sought to examine the effect of the biocatalytic activity of the enzyme on the fluorescence characteristics of the synthesized NCs and to determine if the detectable limit varied between the different synthesis products.

For practical detection of dsDNA, the digestion of dsDNA by DNAse 1:AuNCs must produce a quantifiable change in fluorescence. Such a change in fluorescence following substrate addition has previously been demonstrated with horseradish peroxidase stabilized AuNCs, wherein a linear decrease in NC fluorescence was observed upon titration of the substrate, hydrogen peroxide.[24] Surprisingly, we were unable to observe a difference in the detection limit between the DNase 1 stabilized Au_8 clusters and the Au_{25} clusters, both clusters show a marked decrease in fluorescence upon the addition of 2 ng/μL of DNA (**Figure 4**). The subsequent addition of DNA results in further quenching of NC fluorescence in a linear fashion. As DNA can also serve as a biomolecular host for AuNC synthesis, a control experiment was conducted wherein 300 ng/μL (150 μg total) of DNA was added to a solution of BSA:Au_{25}NCs and no fluorescence quenching was observed for the BSA:Au_{25}NCs upon the addition of DNA (**Figure 5**). Clearly, the DNA mediated quenching of DNase 1:AuNC fluorescence was indeed caused by substrate/enzyme interaction between DNA and DNase 1.

In summary, we have been able to create a multifunctional bio-nano hybrid system. Utilizing the reducing and metal stabilizing properties of proteins for metal nanoclusters, we were able to synthesize blue (Au_8) and red (Au_{25}) emitting DNase 1 :AuNCs in addition to DNase 1 stabilized AuNCs containing mixed populations of both Au_8 and Au_{25} clusters in a concentration dependant fashion. All of the DNase 1:AuNC synthesis products retain the endodeoxyribonuclease activity of the native enzyme and are able to detect a lower limit of 2 μg/mL of DNA . This limit of detection (LOD) is relevant to real world applications in RNA analysis since the DNA contamination in such samples can be up to 10 μg/ml, which is fivefold higher than our LOD. The synthesized DNase 1: NCs could be potentially used for simultaneous detection and digestion of contaminating DNA in RNA isolation process. [26-29]

REFERENCES

[1] J. Xie, *et al.*, "Protein-directed synthesis of highly fluorescent gold nanoclusters," *J Am Chem Soc*, vol. 131, pp. 888-9, Jan 28 2009.

[2] D. M. Chevrier, *et al.*, "Properties and applications of protein-stabilized fluorescent gold nanoclusters: short review," *Journal of Nanophotonics*, vol. 6, pp. 064504-1, 2012.

[3] L. Shang, *et al.*, "Ultra-small fluorescent metal nanoclusters: Synthesis and biological applications," *Nano Today*, vol. 6, pp. 401-418, Aug 2011.

[4] J. Zheng, *et al.*, "Highly fluorescent noble-metal quantum dots," *Annu Rev Phys Chem*, vol. 58, pp. 409-31, 2007.

[5] J. Zheng, *et al.*, "Highly fluorescent, water-soluble, size-tunable gold quantum dots," *Phys Rev Lett*, vol. 93, p. 077402, Aug 13 2004.

[6] J. P. Wilcoxon, *et al.*, "Photoluminescence from nanosize gold clusters," *Journal of Chemical Physics*, vol. 108, pp. 9137-9143, Jun 1 1998.

[7] G. Wang, *et al.*, "Near-IR luminescence of monolayer-protected metal clusters," *J Am Chem Soc*, vol. 127, pp. 812-3, Jan 26 2005.

[8] C. T. Chen, *et al.*, "Glutathione-bound gold nanoclusters for selective-binding and detection of glutathione S-transferase-fusion proteins from cell lysates," *Chem Commun (Camb)*, pp. 7515-7, Dec 28 2009.

[9] D. Hu, *et al.*, "Highly selective fluorescent sensors for Hg(2+) based on bovine serum albumin-capped gold nanoclusters," *Analyst*, vol. 135, pp. 1411-6, Jun 2010.

[10] L. Shang, *et al.*, "Facile preparation of water-soluble fluorescent gold nanoclusters for cellular imaging applications," *Nanoscale*, vol. 3, pp. 2009-14, May 2011.

[11] L. Hu, *et al.*, "Highly sensitive fluorescent detection of trypsin based on BSA-stabilized gold nanoclusters," *Biosens Bioelectron*, vol. 32, pp. 297-9, Feb 15 2012.

[12] L. Shang, *et al.*, "Facile synthesis of fluorescent gold nanoclusters and their application in cellular imaging," *Colloidal Nanocrystals for Biomedical Applications Vii*, vol. 8232, 2012.

[13] P. H. Chan, *et al.*, "Photoluminescent Gold Nanoclusters as Sensing Probes for Uropathogenic Escherichia coli," *PLoS One*, vol. 8, p. e58064, 2013.

[14] H. Chen, *et al.*, "Characterization of a fluorescence probe based on gold nanoclusters for cell and animal imaging," *Nanotechnology*, vol. 24, p. 055704, Feb 8 2013.

[15] H. Zhang, *et al.*, "Facile preparation of glutathione-stabilized gold nanoclusters for selective determination of chromium (III) and chromium (VI) in environmental water samples," *Anal Chim Acta*, vol. 770, pp. 140-6, Apr 3 2013.

[16] T. Hasobe, *et al.*, "Photovoltaic cells using composite nanoclusters of porphyrins and fullerenes with gold nanoparticles," *J Am Chem Soc*, vol. 127, pp. 1216-28, Feb 2 2005.

[17] H. Wei, *et al.*, "Lysozyme-stabilized gold fluorescent cluster: Synthesis and application as Hg(2+) sensor," *Analyst*, vol. 135, pp. 1406-10, Jun 2010.

[18] H. Kawasaki, *et al.*, "ph-Dependent Synthesis of Pepsin-Mediated Gold Nanoclusters with Blue Green and Red Fluorescent Emission," *Advanced Functional Materials*, vol. 21, pp. 3508-3515, Sep 23 2011.

[19] X. Le Guevel, *et al.*, "Synthesis and characterization of human transferrin-stabilized gold nanoclusters," *Nanotechnology*, vol. 22, p. 275103, Jul 8 2011.

[20] C. L. Liu, *et al.*, "Insulin-directed synthesis of fluorescent gold nanoclusters: preservation of insulin bioactivity and versatility in cell imaging," *Angew Chem Int Ed Engl*, vol. 50, pp. 7056-60, Jul 25 2011.
[21] Y. Chen, *et al.*, "Papain-directed synthesis of luminescent gold nanoclusters and the sensitive detection of Cu(2+)," *J Colloid Interface Sci*, vol. 396, pp. 63-8, Apr 15 2013.
[22] A. R. Garcia, *et al.*, "Human insulin fibril-assisted synthesis of fluorescent gold nanoclusters in alkaline media under physiological temperature," *Colloids Surf B Biointerfaces*, vol. 105, pp. 167-72, May 1 2013.
[23] X. D. Zhang, *et al.*, "In vivo renal clearance, biodistribution, toxicity of gold nanoclusters," *Biomaterials*, vol. 33, pp. 4628-38, Jun 2012.
[24] F. Wen, *et al.*, "Horseradish Peroxidase Functionalized Fluorescent Gold Nanoclusters for Hydrogen Peroxide Sensing," *Analytical Chemistry*, vol. 83, pp. 1193-1196, Feb 15 2011.
[25] T. H. Chen and W. L. Tseng, "(Lysozyme type VI)-stabilized Au8 clusters: synthesis mechanism and application for sensing of glutathione in a single drop of blood," *Small*, vol. 8, pp. 1912-9, Jun 25 2012.
[26] M. Pruvost, *et al.*, "Minimizing DNA contamination by using UNG-coupled quantitative real-time PCR on degraded DNA samples: application to ancient DNA studies," *Biotechniques*, vol. 38, pp. 569-575, Apr 2005.
[27] S. Tondeur, *et al.*, "Overcoming bacterial DNA contamination in real-time PCR and RT-PCR reactions for LacZ detection in cell therapy monitoring," *Molecular and Cellular Probes*, vol. 18, pp. 437-441, Dec 2004.
[28] J. L. Matthews, *et al.*, "Persistent DNA contamination in competitive RT-PCR using cRNA internal standards: identity, quantity, and control," *Biotechniques*, vol. 32, pp. 1412-4, 1416-7, Jun 2002.
[29] M. Anez-Lingerfelt, *et al.*, "Reduction of DNA contamination in RNA samples for reverse transcription-polymerase chain reaction using selective precipitation by compaction agents," *Analytical Biochemistry*, vol. 384, pp. 79-85, Jan 1 2009.